Extracting topographic characteristics of landforms typical of Canadian agricultural landscapes for agri-environmental modeling. I. Methodology

Sheng Li[1], David A. Lobb[1], Brian G. McConkey[2], R. A. MacMillan[3], Alan Moulin[4], and Walter R. Fraser[5]

[1]Department of Soil Science, University of Manitoba, Winnipeg, Manitoba, Canada R3T 2N2 (e-mail:shenglcn@yahoo.com); [2]Semiarid Prairie Agricultural Research Centre, Agriculture and Agri-Food Canada, Swift Current, Saskatchewan, Canada S9H 3X2; [3]ISRIC – World Soil Information, Wageningen, the Netherlands; [4]Brandon Research Centre, Agriculture and Agri-Food Canada, Brandon, Manitoba, Canada R7A 5Y3; and [5]Land Resource Unit, Agriculture and Agri-Food Canada, Winnipeg, Manitoba, Canada R3T 2N2.
Received 9 July 2010, accepted 4 February 2011.

Li, S., Lobb, D. A., McConkey, B. G., MacMillan, R. A., Moulin, A. and Fraser, W. R. 2011. **Extracting topographic characteristics of landforms typical of Canadian agricultural landscapes for agri-environmental modeling. I. Methodology**. Can. J. Soil Sci. **91**: 251–266. Soil and topographic information are key inputs for many agri-environmental models and there are linkages between soil and topography at the field scale. A major source of soil data is soil databases established based on field soil survey. Although both soil and topographic information are recorded in field soil surveys, the nominal nature of the topographic data has limited their use in agri-environmental models. In this study, we developed a methodology to extract various topographic derivatives and to classify the landscape into landform elements with distinctive topographic characteristics based on detailed analyses of fine resolution digital elevation models. Data obtained from these analyses were used to calculate a representative two-dimensional hillslope of five segments, each with a defined length and slope gradient. A set of modal hillslopes was developed to describe topographic variability. Additional topographic parameters, ratios and indices were calculated to reflect different aspects of topographic characteristics and also to build connections between different agri-environmental models. In particular, a topographic complexity index was developed as a quantitative measure of the degrees of divergence and convergence. This paper describes the methodology using one site as an example. Application of this methodology to other landforms in agricultural land of Canada is reported in a companion paper.

Key words: Topography, landscape segmentation, landform, hillslope

Li, S., Lobb, D. A., McConkey, B. G., MacMillan, R. A., Moulin, A. et Fraser, W. R. 2011. **Extraction des particularités topographiques du relief type des zones agricoles canadiennes en vue d'une modélisation agro-environnementale. I. Méthodologie**. Can. J. Soil Sci. **91**: 251–266. Les données topographiques et celles sur le sol sont indispensables à maints modèles agro-environnementaux; sur le terrain, elle font la jonction entre le sol et le relief. Bon nombre des données sur le sol émanent de bases de données reposant sur des levés pédologiques. Bien que de tels levés incluent des données sur le sol et le relief, la nature nominale des données topographiques en limite l'usage dans les modèles agro-environnementaux. Les auteurs ont élaboré une méthode pour extraire divers dérivés topographiques et classer le relief en plusieurs éléments présentant des caractéristiques topographiques précises, d'après une analyse détaillée des modèles numériques de hauteurs à haute résolution. Les données issues de cette analyse ont permis de calculer la pente bidimensionnelle représentative de cinq segments, chacun d'une longueur et d'un gradient de pente déterminés. Ensuite, les auteurs ont créé un jeu de pentes modales qui décrit la variabilité du relief. Ils ont calculé d'autres paramètres topographiques, ratios et indices afin de refléter diverses facettes des paramètres topographiques et d'établir les liens entre plusieurs modèles agro-environnementaux. Ils ont notamment développé un index de la complexité du relief en fonction du degré de divergence ou de convergence mesuré quantitativement. Cet article décrit la méthodologie employée en prenant un site comme exemple. L'application de cette méthode à d'autres types de relief sur les terres agricoles du Canada fera l'objet d'un second article.

Mots clés: Topographie, segmentation du relief, relief, pente

Soil and topography are interlinked in nature. Soil genesis is a function of five major factors (parent material, climate, biota, topography and time), of which, topography is usually the driving factor at the field scale (Brady and Well 2002). At the field scale, soil series are correlated with slope positions, resulting in a sequence

Abbreviations: **AEI**, agri-environmental indicator; **CST**, crest; **DEP**, depression; **DEM**, digital elevation model; **DSM**, digital soil mapping; **LE**, landform element; **LOW**, lowerslope; **MID**, midslope; **PA**, area percentage; **PL**, length percentage; **RUSLE**, Revised Universal Soil Loss Equation; **TCI**, topographic complexity index; **UPS**, upperslope; **SLC**, Soil Landscape of Canada

along hillslopes (catena). Linkages between soil and topography have been demonstrated in numerous studies (e.g., Pennock et al. 1987, 1994; Li et al. 2008; Qin et al. 2009).

Both soil and topography are key information in many agri-environmental models. Most agri-environmental models require quantitative inputs for soil parameters (e.g., texture, soil organic carbon content) characterized by depth, at the scale of the processes to be simulated. For regional, national and continental studies, soil information is usually obtained from soil databases published and maintained by government agencies such as Agriculture and Agri-Food Canada (AAFC) in Canada, the Natural Resources Conservation Service (NRCS) in the USA and the Institute for Environment and Sustainability of the Joint Research Center (JRC) in Europe. These databases were compiled from data collected during soil surveys. Soil survey maps delineate soil units with attribute tables of soil properties. In detailed field soil surveys, topographic information associated with soil units (e.g., dominant landforms, slope gradient classes) is also recorded. Although mostly nominal in nature, this topographic information characterizes the range of topographic attributes (e.g., relief, slope length, slope gradient and slope curvature). Furthermore, it summarizes expert knowledge about the linkages between soil and topography, i.e., the topographic context of soils observed in the field. Only some of this topographic information is incorporated into national or continental soil databases.

Data for soil properties in soil databases often meet the requirements of model simulation, but data for topographic information generally cannot be used directly for modeling purposes. Therefore, topographic maps or digital elevation models (DEM) are often used to obtain topographic data. Various algorithms have been developed to extract topographic derivatives from DEMs through terrain analysis (Wilson and Gallant 2001). These extracted topographic derivatives have been used in a wide range of hydrological, geomorphological and ecological applications and to classify landscapes into landform elements through landscape segmentation (e.g., Band 1986; Irwin 1997; Pennock et al. 1987, 1994; Burrough et al. 2000; MacMillan et al. 2003; Qin et al. 2009). Digital elevation models have also been used to facilitate soil survey based on the correlation of landform attributes and elements with soil properties in the landscape (e.g., Moore et al. 1993; Zhu et al. 1997, 2001). Most of these studies focused on individual sites and were not linked to an operational soil database.

Few large scale studies utilize soil databases and DEMs. Kirkby et al. (2008) used remote sensed DEMs as topographic inputs and the European soil database as soil inputs to estimate long-term average erosion rates at 1 km resolution in Europe. In their study, the DEMs and soil databases were analyzed separately and valuable information about the linkages between soil and topography in the original soil surveys was not incorporated in the analysis. Clearly, the nominal nature of the topographic information contained in soil surveys around the world has limited its use in agri-environmental models. On the other hand, advances in DEM data collection and terrain analysis technologies have facilitated landform analyses, such as landscape segmentation. If it can be assumed that a given landform in a soil database has consistent topographic characteristics, then these topographic characteristics can be obtained through detailed terrain analyses of representative sites.

In Canada, the National Soil Database is built upon the Soil Landscape of Canada (SLC) polygons for the entire land mass of Canada (AAFC 2007). The SLC are based on soil survey maps recompiled at 1:1 million scale. The size of the SLC polygons generally varies from 10 000 ha to 1 000 000 ha. Soil Landscape of Canada polygons are characterized by a standard set of attributes, including the dominant soils, landform type (termed surface form in SLC) and slope classes. Detailed soil profile data are linked to the SLC polygons via the soil name. Topography within SLC polygons is defined by a combination of landform type and slope class. There are 10 landform types and six slope classes, but in the agricultural region of Canada, only 8 of the 10 landform types are present, for a total of 21 combinations of landform type and slope class.

Since the release of the first version of the SLC database in 1991, it has been used in a variety of regional and national studies (e.g., McConkey et al. 2003; Rochette et al. 2008). In 1993, Agriculture and Agri-Food Canada launched the National Agri-Environmental Health Analysis and Reporting Program (NAHARP). The National Agri-Environmental Health Analysis and Reporting Program is aimed at providing science-based agri-environmental information that can guide policy and program design (Lefebvre et al. 2005). The core of NAHARP is a set of agri-environmental indicators (AEI) that integrate biophysical information (on soil, climate and landscape) with land use and farm management data. These AEIs were calculated on the SLC polygon level. Many AEIs were simplified versions of established agri-environmental models (e.g., the Revised Universal Soil Loss Equation) that require soil data along a two-dimensional (horizontal and vertical) hillslope. As a result, there is a need to convert the landform information (landform type and slope class) in the National Soil Database into quantitatively defined hillslopes.

In a previous study in the province of Alberta, a framework was established to approximate the topography of a landscape using a representative two-dimensional hillslope, consisting of four segments, each with defined length and slope gradient (MacMillan and Pettapiece 2000). The representative hillslope were computed based on landscape segmentation analyses at individual sites using fine resolution DEMs. The framework has proven to be an efficient way to convert

landform information into quantitative topographic data, and the representative hillslope data were used in the current NAHARP (Lefebvre et al. 2005). However, questions have been raised regarding the accuracy of the representative hillslopes, particularly because the sites were all in one province (MacMillan and Pettapiece 2000). Also, there is growing concern over the uncertainties of agri-environmental indicators, which is directly related to the variability in topography (e.g., slope length, gradient and relief of hillslopes). A single representative hillslope does not quantify topographic variability. Furthermore, many agri-environmental processes are interrelated (e.g., soil erosion and soil organic carbon sequestration). As an integrated product, connections between different agri-environmental indicators should be established in NAHARP. A single representative hillslope does not provide enough information for this purpose. Therefore, there is also a need to include additional topographic parameters to build the connections.

The objective of this study is to develop a method ology to extract topographic characteristics based on terrain analysis of fine-resolution DEMs. This methodology was developed as part of the NAHARP project to facilitate agri-environmental modeling. The methodology will be applied on sites representative of landforms typical of Canadian agricultural landscapes. The goal is to establish a comprehensive topographic model for each landform in the SLC database so that nominal topographic information (landform type and slope class) stored in the SLC database can be systematically converted into quantitative topographic data that can be used in agri-environmental modeling. In this paper, we describe the methodology using one site as an example. Application of this methodology to other landforms in the SLC database is reported in a subsequent paper.

TERRAIN ANALYSES AND LANDSCAPE SEGMENTATION

The LandMapR toolkit was developed by MacMillan (2003) to classify landscapes into landform elements (LE). The analysis uses three stand-alone subprograms sequentially (FlowMapR for flow topology analysis, FormMapR for deriving terrain derivatives, and FacetMapR for classification of landform elements). Detailed descriptions about the algorithms and methodology used in the LandMapR programs can be found in the original publications (MacMillan et al. 2000; MacMillan 2003). To illustrate the procedure, the Provost site in the previous study (MacMillan and Pettapiece 2000) is presented here as an example (Fig. 1a). Landform of the area is classified as high relief undulating. The raw topographic data of the Provost site were obtained using a Total Station (an instrument integrates a electronic theodolite and an electronic distance meter for topographic survey) and subsequently interpolated (ArcView Inverse Distance Weighted interpolation) and filtered (3×3 mean filtered twice and 5×5 mean filtered twice) to obtain a 5-m square-grid DEM with 184 rows and 187 columns. Detailed descriptions about the site and DEM data acquisition can be found in MacMillan and Pettapiece (2000). Undulating landform occupies about 49% of Canadian agricultural land (AAFC 2007). However, the Provost site was chosen not because it is representative of Canadian agricultural landscapes but because it has a range of topographic features and a simple drainage pattern so that the methodology can be clearly shown.

Flow Topology

The FlowMapR subprogram defines flow topology between adjacent points (grid nodes, each representing a cell) in the DEM. Simulated networks of surface water flow are calculated using a simple D8 algorithm (allowing water to flow from the central point to only one of its eight adjacent points). Local watersheds (each pit defines a local watershed) and the upslope catchment area for each point (upslope points count) are determined based on the flow topology (Fig. 1a, b). The flow analyses are then repeated on an inverted version of the DEM (turning the DEM upside down) to compute downslope catchment area (upslope points count in the inverted DEM) for each point (Fig. 1c). By processing both the original and inverted DEMs, the divergence (the inverted DEM) and convergence (the original DEM) water flows in convex and concave areas, respectively, have been explicitly taken into account (Fig. 1a, b, c).

In a three-dimensional (3D) field, each flow path starts from a peak and ends at a pit (referred to as full flow path, herein). However, due to divergent and convergent water flow in convex (associated with peaks and ridges) and concave (associated with pits and channels) areas, respectively, the effective flow path (in the overland flow area) in two-dimensional (2D) models is defined as from ridge to channel (e.g., Foster 2004). In the second subprogram, FormMapR, points with upslope and downslope catchment area (in the original and inverted DEM, respectively) greater than a user specified threshold value are recorded as channel and ridge points, respectively (Fig. 1b, c, d). Therefore, for each grid point in the DEM, its associated pit, peak, channel and ridge points can be determined. Thus, both the full and effective flow path are defined (Fig. 1d).

Topographic Derivatives

A set of topographic derivatives are calculated in FormMapR (some are listed Table 1). Simple statistical analyses were conducted to summarize these topographic derivatives (Table 1). These statistics were calculated using each point as one sample and, therefore, were area weighted values. The mean and 50th percentile (median) values show the central tendency, whereas the standard deviation (SD) and percentile values (Fig. 2a) indicate the variability of these

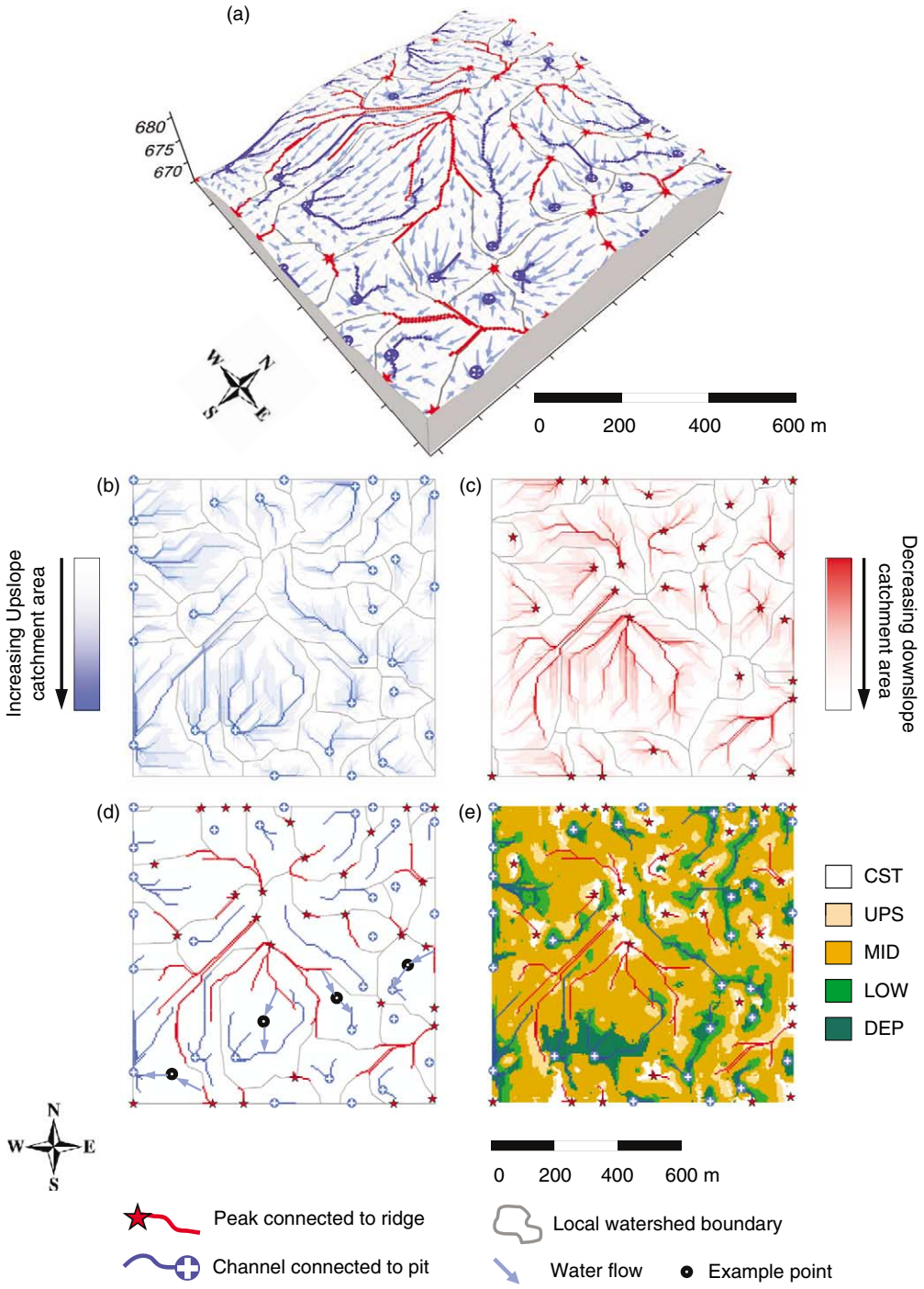

Fig. 1. Results for the Provost site: (a) Three-dimensional view showing the ridges, channels, local watershed boundaries and water flow directions; (b) upslope catchment area for each point and local watershed boundaries derived from the original DEM; (c) downslope catchment area for each point and the boundaries of local watersheds derived from the inverted DEM; (d) ridges and channels defined for the site and some example effective-flow-paths; and (e) final landscape segmentation results.

topographic derivatives. For example, the 10th percentile slope gradient (0.9%) can be interpreted as 10% of the points (i.e., area) had slope gradient equal to or less than 0.9%. The boundary effect at the edges of DEM resulted in incomplete watersheds (e.g., two small watersheds near the northeast corner in Fig. 1d). As a result, the flow path lengths calculated for the points located near the DEM edges were incomplete (too

Table 1. Statistics of selected topographic derivatives (area-weighted) obtained from FormMapR outputs[z]

Parameter	Symbol	Mean	SD	Percentiles				
				10th	25th	50th	75th	90th
Slope gradient (%)	SG	2.6	1.3	0.9	1.5	2.4	3.3	4.4
Profile curvature [degree (100 m)$^{-1}$]	PrCur	0.0	5.4	−6.4	−2.9	0.0	3.1	6.6
Plan curvature [degree (100 m)$^{-1}$]	PlCur	0.2	5.0	−5.7	−2.6	0.1	3.0	6.3
Wetness index	WI	4.7	1.5	3.1	3.7	4.5	5.4	6.6
Full-flow-path (peak to pit) length (m)	L_{p2p}	309	142	135	203	287	406	489
Full-flow-path (peak to pit) relief (m)	Z_{p2p}	6.9	3.5	2.3	3.9	6.6	9.7	10.0
Effective-flow-path (ridge to channel) length (m)	L_{r2c}	142	62	77	100	129	168	223
Effective-flow-path (ridge to channel) relief (m)	Z_{r2c}	3.5	1.9	1.5	2.2	3.2	4.7	6.2
Effective-flow-path (ridge to channel) gradient (%)	S_{r2c}	2.5	0.7	1.5	2.1	2.5	2.9	3.4
Effective-flow-path (ridge to channel) LS-factor	LS	0.50	0.18	0.26	0.38	0.49	0.62	0.75

[z]Values calculated for the Provost site. To reduce the boundary effect, nine rows or columns along each edge of the DEM were eliminated from the statistical analyses.

short). To reduce this boundary effect, nine rows or columns of the data along each edge of the DEM (approximately 10% of the total numbers of rows and columns of the DEM, respectively) were eliminated from the statistical analyses. This was considered adequate given the watershed size of the site.

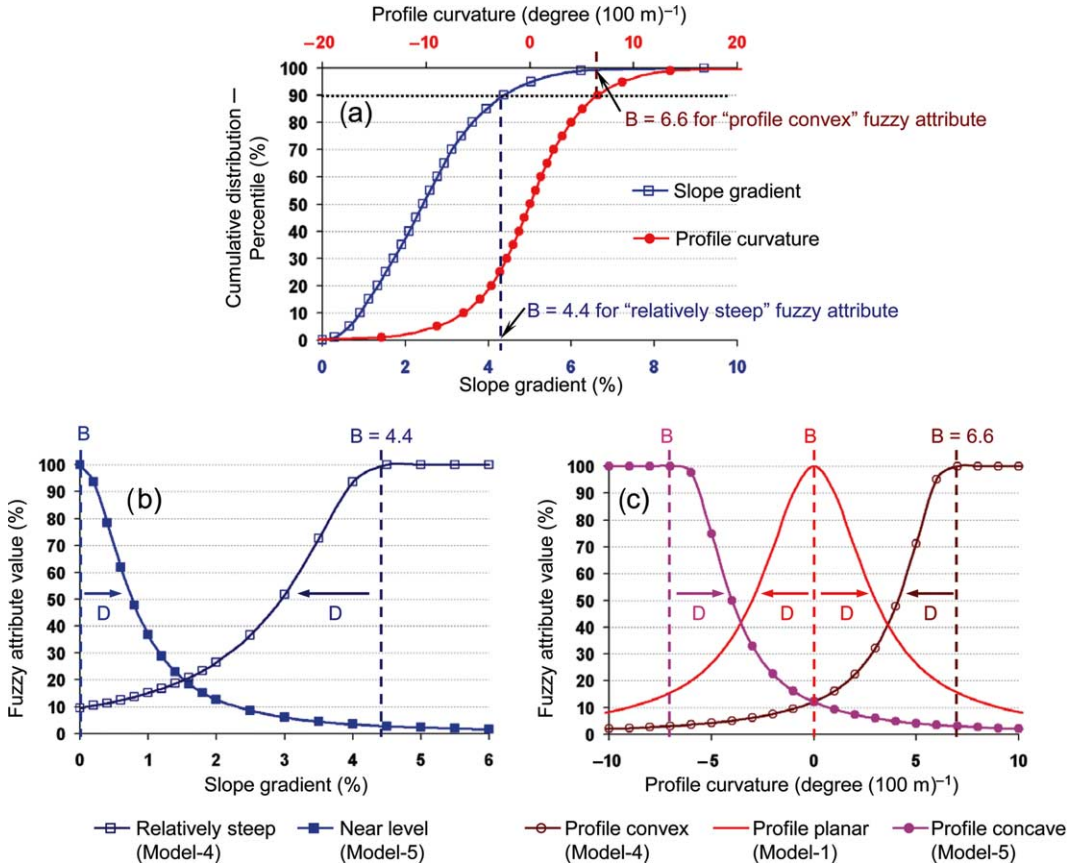

Fig. 2. Illustration of the procedures developed to determine boundary (B) and dispersion (D) parameters of the fuzzy models using the distributions (percentiles) of topographic derivatives: (a) cumulative distribution (standardized to from 0 to 100) of the slope gradient and profile curvature; (b) fuzzy models for the "relatively steep" and "near level" fuzzy attributes, using slope gradient as input data; and (c) fuzzy models for the "profile convex", "profile planar" and "profile concave" fuzzy attributes, using profile curvature as input data. The values of B and D in (b) and (c) are determined using equations defined in Table 3. B values of the "relatively steep" and "profile convex" fuzzy attributes for the Provost site are shown as examples.

It should be noted that the flow path length for a given point was calculated as the sum of the horizontal distances from that point to its associated ridge and channel points (the effective flow path length) or its associated peak and pit points (the full flow path length). A more precise approach is probably to trace the water flow, point by point, up to the ridge or peak point and down to the channel or pit point, calculating the cumulative lengths crossing each cell and using these cumulative lengths as the final flow path lengths. This approach is computationally inefficient and impractical for large DEMs. Furthermore, the D8 algorithm allows water flow in only one direction so that simulated flow may follow a zigzag path in the DEM. As a result, the point-by-point tracing approach may overestimate flow path length depending on the density of the grid points in the DEM. The approach taken in this study is a simplification, and may underestimate flow path length as affected by the degrees of divergence and convergence. On topographically simple landscapes (little divergence or convergence flow), the underestimation is negligible (e.g., Fig. 3a), but on topographically

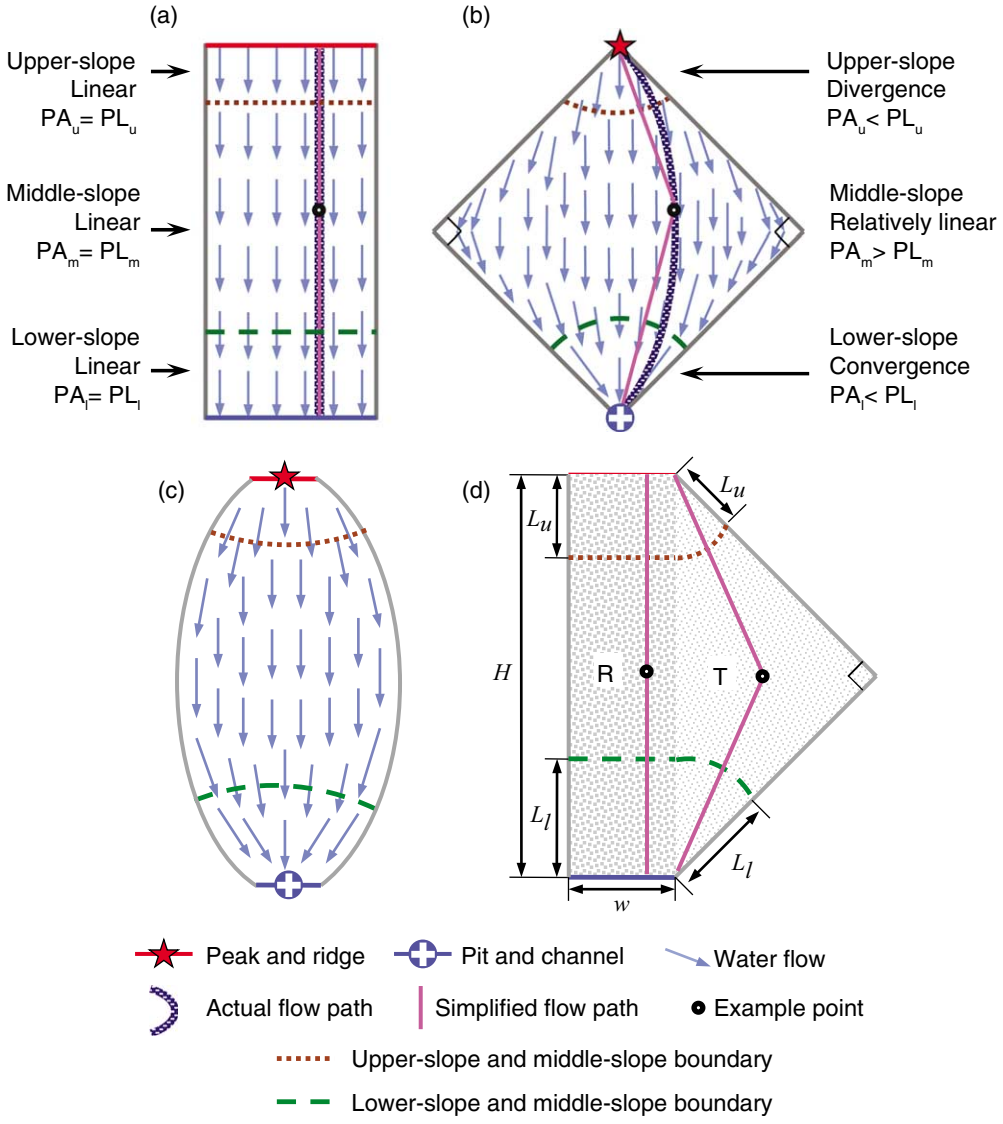

Fig. 3. (a) the scenario of a landscape with no divergence or convergence and, therefore, no difference between area percentages (PA) and length percentages (PL) for the same landform elements (hillslope segments in the context of a hillslope); (b) the scenario of a landscape with the highest divergence and convergence and, therefore, different PAs and PLs for the same landform elements; (c) a general scenario that can be theoretically represented by (d) a combination of the two extreme scenarios shown in (a) and (b), consisting of a rectangular component (R) and a triangular component (T).

complex landscapes (high divergence and convergence), the underestimation could be substantial (e.g., Fig. 3b). However, since the divergent and convergent water flows have largely been taken into account by defining ridges and channels, the underestimation of the effective flow path length (ridge to channel) is expected to be low.

Landscape Segmentation

FacetMapR classifies points into landform elements based on topographic derivatives (Table 2). Six of the topographic derivatives calculated by FormMapR, including slope gradient, profile and plan curvatures, wetness index and relative positions of points in the effective flow path (ridge to channel) and full flow path (peak to pit). These are used to determine the values of a set of fuzzy attributes for each point based on specified fuzzy models (Table 3). Three of the five fuzzy models (Models 1, 4, and 5) defined by Burrough et al. (1992) were used. All three fuzzy models share a common equation:

$$MF_x = \frac{1}{1 + [(x - B)/D]^2} \quad (1)$$

where MF_x is the fuzzy membership value, x is the value of the topographic derivative, and B and D are the boundary and dispersion parameters, respectively. The value of the fuzzy attribute (F_x) is calculated as:

$$\text{Model 1: } F_x = 100MF_x \quad (2)$$

$$\text{Model 4: } F_x = \begin{cases} 100MF_x & (x < B) \\ 100 & (x \geq B) \end{cases} \quad (3)$$

$$\text{Model 5: } F_x = \begin{cases} 100 & (x \leq B) \\ 100MF_x & (x > B) \end{cases} \quad (4)$$

The values of the fuzzy attributes (from 0 to 100) calculated for a given point can be interpreted as the degree to which a point exhibits these fuzzy attributes as illustrated in Fig. 2b and c (e.g., a point with high slope gradient will have a high value for the "relatively steep" fuzzy attribute but low value for the "level" fuzzy attribute).

The source topographic derivatives, the type of fuzzy model and the values of B and D used to compute each fuzzy attribute are obtained from a user defined fuzzy attribute rule file (A-rule file). There are several default A-rule files, which were developed based on sites located in Alberta, Canada (MacMillan 2003), where the landscapes feature gentle slopes. These A-rule files (i.e., the values of B and D) may not be optimal for level or high relief landscapes in other parts of Canada. For example, in one of these A-rule files, a B value of 2% and a D value of 1% are used to calculate the "relatively steep" fuzzy attribute from slope gradient. Therefore, a point with slope gradient greater than 2% is assigned a value of 1 for the "relatively steep" fuzzy attribute. For a high relief site, the majority of points could have greater than 2% slope gradient (e.g., Li et al. 2010). Since all points with $>2\%$ slope gradient are assigned a value of 1, this A-rule file cannot separate the steepest points (e.g., with slope gradient $>20\%$) from those much less steep ones (e.g., with slope gradient at about 3%).

As mentioned above, the purpose of landscape analysis is to classify the points into landform elements and, therefore, what is important is to distinguish points from each other in a given field. The value of a point relative to those of other points is what determines which landform element it belongs to, and this cannot be achieved through any single A-rule file. It was therefore recommended that different A-rule files should be used for sites with very different local relief (MacMillan 2003). However, the methodology developed in this study is designed for the entire country of Canada, which has a wide range of landscapes with variable local relief. It is unrealistic to develop A-rule files for each landform. On the other hand, using different A-rule files raises questions about the consistency of the methodology. Therefore, we defined the values of B and D in the A-rule file based on the distributions (percentiles) of the topographic derivatives (Table 3, Fig. 2). This ensured that points with substantially different values of topographic derivatives can be effectively separated in the resulting fuzzy attributes. The consistency of the rules was maintained in that the algorithms used to generate the two parameters, B and D, were always the same for the same fuzzy attributes.

Table 2. General characteristics of the five landform elements defined in this study

Landform Element (LE)		Topographic attributes			Position	
Name	Code	Slope gradient	Profile curvature	Plan curvature	Ridge to channel	Peak to pit
Crest	CST	Level	Convex to linear	Convex	Near ridge	Near peak
Upperslope	UPS	Moderate	Convex	–	Between ridge and half[z]	–
Midslope	MID	Steep	Linear	Linear	Near half[z]	Near middle[y]
Lowerslope	LOW	Moderate	Concave	–	Between channel and half[z]	–
Depression	DEP	Level	Concave to linear	Concave	Near channel	Near pit

[z]Half means the halfway point of the effective-flow-path (ridge to channel).
[y]Middle means the middle point of the full-flow-path (peak to pit).

Table 3. Fuzzy attributes and their associated A-rules and C-rules defined in this study for landscape segmentation

Fuzzy attribute	Source topographic derivative	Fuzzy model (A-rule)[z]			Weight for landform element (C-rule)[y]				
		Type	B	D	CST	UPS	MID	LOW	DEP
Relatively steep	Slope gradient	4	P_{90}	$(P_{90}-P_{50})/2$	0	20	30	20	0
Near level	Slope gradient	5	0	$P_{25}/2$	10	0	0	0	10
Profile convex	Profile curvature	4	P_{90}	$(P_{90}-P_{65})/2$	15	20	0	0	0
Profile planar	Profile curvature	1	0	$(P_{75}-P_{25})/2$	15	0	25	0	15
Profile concave	Profile curvature	5	P_{10}	$(P_{35}-P_{10})/2$	0	0	0	20	15
Plan convex	Plan curvature	4	P_{90}	$(P_{90}-P_{65})/2$	10	0	0	0	0
Plan planar	Plan curvature	1	0	$(P_{75}-P_{25})/2$	0	0	10	0	0
Plan concave	Plan curvature	5	P_{10}	$(P_{35}-P_{10})/2$	0	0	0	0	10
High wetness	Wetness index	4	P_{90}	$(P_{90}-P_{50})/2$	0	0	0	20	20
Low wetness	Wetness index	5	P_{10}	$(P_{50}-P_{10})/2$	20	20	0	0	0
Near ridge	Percent relief to channel	4	100	$(100-P_{75})/2$	10	30	0	0	0
Near half	Percent relief to channel	1	50	$(P_{75}-P_{25})/2$	0	10	25	10	0
Near channel	Percent relief to channel	5	0	$P_{25}/2$	0	0	0	30	10
Near peak	Percent relief to pit	4	100	$(100-P_{75})/2$	20	0	0	0	0
Near middle	Percent relief to pit	1	50	$(P_{75}-P_{25})/2$	0	0	10	0	0
Near pit	Percent relief to pit	5	0	$P_{25}/2$	0	0	0	0	20

[z]B and D are the boundary and dispersion parameters used in the fuzzy model. P_x denotes the xth percentile of the source topographic derivative.
[y]CST, crest; UPS, upperslope; MID, midslope; LOW, lowerslope; DEP, depression. The sum of weights for each landform element equals 100.

Another fuzzy rule file (C-rule file) is used to define the landform elements and the weights of fuzzy attributes for each landform element (Table 3). For each point in the DEM, the values of fuzzy attributes are multiplied by their respective weights and the sum of the products is the score for that landform element. Thus, each point has a set of scores corresponding to the landform elements. Individual points are assigned (classified) to the landform element that has the highest score among all landform elements. Several default C-rule files are distributed with the LandMapR program (MacMillan 2003). In these default C-rule files, landform elements are determined at two levels. At the lower level, 15 basic landform elements (15 LEs) are determined, which provide considerable detail about the landscape. However, differences between many of these 15 LEs are subtle, which often result in isolated points in complicated landscapes and, therefore, noisy maps (MacMillan 2003). To obtain more integrated and meaningful classification results, at a higher level, the 15 LEs are grouped into four major landform elements (4 LEs). This two-level system has been used by other researchers in landscape segmentation studies (e.g., Pennock 2001). However, after the grouping, topographic characteristics of the 4 LEs become ambiguous since each 4 LE contains different combinations of the original 15 LEs, and any one combination may have inconsistent topographic characteristics.

To overcome the shortcomings of the two-level system, in this study, a new C-rule file was developed, in which five landform elements with distinct topographic characteristics – crest (CST), upperslope (UPS), midslope (MID), lowerslope (LOW) and depression (DEP) – were classified in one step (Table 2). In this new C-rule file, the weights of fuzzy attributes assigned to each landform element corresponded to local topography (e.g., slope gradient and slope curvature) and relative position in the full- and effective-flow paths (Table 3). In particular, the UPS, MID and LOW were designed to reflect profile topography along a two-dimensional hillslope, whereas the CST and DEP were designed to reflect the additional divergence and convergence in three dimensions, especially around peak and pit points, respectively (Tables 2 and 3). As a result, CST and DEP were considered as portions of upperslope and lowerslope where divergence and convergence were the strongest, respectively, as illustrated for the Provost site in Fig. 1e. Overall, the five landform elements were considered adequate to characterize the major topographic variability in three dimensions.

CHARACTERIZING THE LANDSCAPE TOPOGRAPHY

Representative Hillslope

With each point in the DEM being classified into five LEs, topographic derivatives can be summarized for each LE (Table 4) using the same statistics as those for the landscape (Table 1). However, these area-weighted topographic derivatives cannot be used directly to derive the two-dimensional hillslope due to divergence and convergence of topography in three dimensions. In particular, the length of each segment (the term "segment" is used for "landform element" in the context of a hillslope, herein) cannot be calculated as the flow path length multiplying the area percentages due to differences between area and length percentages related to divergence and convergence (Fig. 3b, c). Therefore, in this study, we developed an algorithm to derive a representative two-dimensional hillslope for the landscape as follows:

Table 4. Point and segment topographic derivatives for the landform elements (hillslope segments)

Topographic attribute	Symbol	Landform element (LE)/hillslope segment (HS)[z]						
		CST	UPS	MID	LOW	DEP	Mean	Sum
Selected point topographic derivatives (area-weighted average)								
Slope gradient (%)	SG	1.5	2.8	2.8	2.5	1.3	2.6	–
Profile curvature [degree (100 m)$^{-1}$]	PrCur	4.2	7.1	−0.2	−7.2	−2.7	0.0	–
Plan curvature [degree (100 m)$^{-1}$]	PlCur	5.9	5.4	0.0	−4.7	−4.3	0.2	–
Wetness index	WI	3.4	3.3	4.6	5.9	7.3	4.7	–
Segment topographic derivatives of the representative hillslope								
Length (m)	L	9	27	67	22	17	–	142
Relief (m)	Z	0.1	0.6	2.1	0.5	0.2	–	3.5
Slope gradient (%)	S	1.3	2.3	3.1	2.3	1.4	2.5	–
Area percentage (%)	PA	7	13	59	11	9	–	100
Length percentage (%)	PL	6	19	47	16	12	–	100
Relief percentage (%)	PZ	3	17	58	15	7	–	100

[z]CST, crest; UPS, upperslope; MID, midslope; LOW, lowerslope; DEP, depression.

(1) Total length (L) and relief (Z) of the hillslope. Since the hillslope is defined for two-dimensional modeling, the mean effective flow path length (L_{r2c}) and relief (Z_{r2c}) were used as the total length and relief, respectively, of the representative hillslope. The term "hillslope" refers to "effective flow path" in the context of two-dimensional topographic descriptions.

(2) Segment length. The boundaries between landform elements were identified and their associated ridge and channel points were located. There were four types

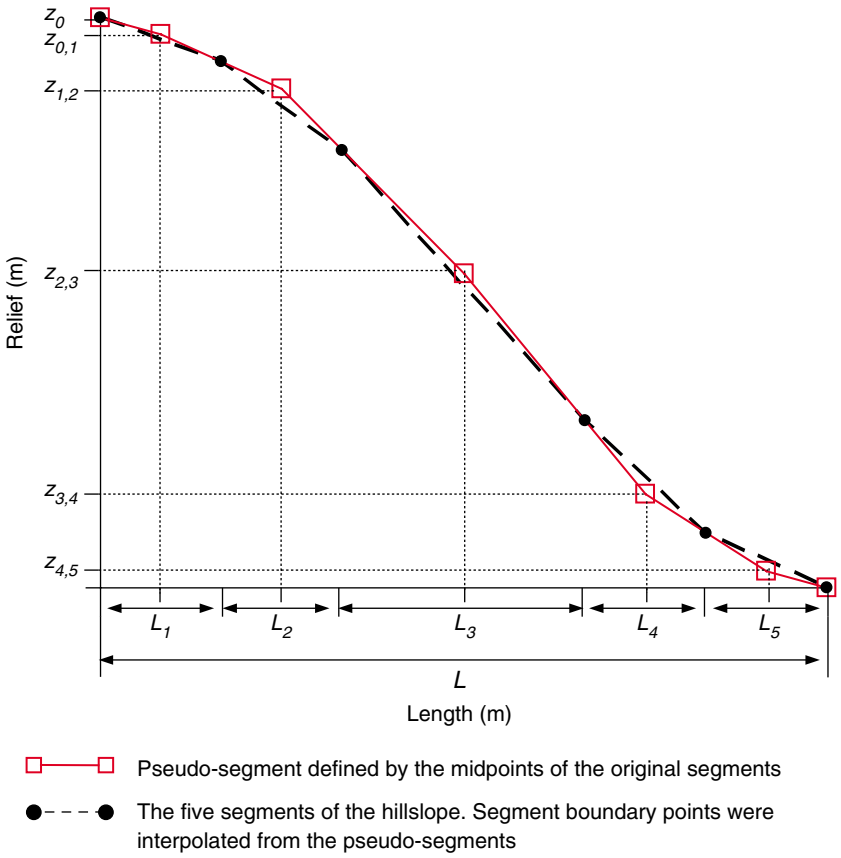

Fig. 4. Illustration of the procedures developed to derive segment reliefs of the representative hillslope and the modal hillslopes from segment lengths, profile curvatures and total hillslope relief.

of boundaries: between crest and upperslope (CST-UPS), between upperslope and midslope (UPS-MID), between midslope and lowerslope (MID-LOW) and between lowerslope and depression (LOW-DEP) landform elements (Fig. 4). The distances between the boundaries and their associated ridge points (for boundaries CST-UPS and UPS-MID) or channel points (for boundaries MID-LOW and LOW-DEP) were calculated and were averaged among each boundary. The numbers of ridge and channel points within each landform element were counted and the mean lengths of the hillslope segments were calculated using the following equations:

$$L_1 = L_{CST-UPS}\frac{NR_1}{NR_1 + NR_2} \tag{5}$$

$$L_2 = L_{UPS-MID} - L_1 \tag{6}$$

$$L_5 = L_{LOW-DEP}\frac{NC_5}{NC_4 + NC_5} \tag{7}$$

$$L_4 = L_{MID-LOW} - L_5 \tag{8}$$

$$L_3 = L - L_1 - L_2 - L_4 - L_5 \tag{9}$$

where L is the total hillslope length (m); L with subscripted numbers 1 to 5 denotes the segment lengths, in sequence, from CST to DEP; L with subscripted text denotes the lengths between boundaries and their associated ridge or channel points; and NR and NC are the numbers of ridge and channel points, respectively, in the landform element (hillslope segment) denoted by their subscripted numbers.

In Eqs. 5 and 7, the lengths of CST and DEP (L_1 and L_5, respectively) were initially calculated from the mean distances between the boundary points (CST-UPS and LOW-DEP, respectively) and their associated ridge or channel points ($L_{\text{CST-UPS}}$ and $L_{\text{LOW-DEP}}$, respectively), then adjusted by factors derived from the numbers of ridge and channel points in CST and UPS (for $L_{\text{CST-UPS}}$) and LOW and DEP (for $L_{\text{LOW-DEP}}$), respectively. These adjustments were applied as CST and DEP were the divergent and convergent portion of the upperslope and lowerslope areas, respectively. Ridge and channel were designed to dissect divergent and convergent areas into two-dimensional hillslopes and, therefore, often extended the CST and DEP (Fig. 1e). As a result, many effective flow paths started from UPS (rather than CST) or ended at LOW (rather than DEP). For these effective flow paths, the lengths for CST or DEP were virtually zero. The $L_{\text{CST-UPS}}$ and $L_{\text{LOW-DEP}}$ did not include these effective flow paths and thus overestimated the overall lengths of CST and DEP. The fractions of those effective flow paths with non-zero-length CST and DEP can be approximated as:

$$\frac{NR_1}{NR_1 + NR_2} \text{ and } \frac{NC_5}{NC_4 + NC_5}, \text{ respectively.}$$

These fractions were used in Eqs. 5 and 7 as adjustment factors to obtain overall means of CST and DEP lengths (L_1 and L_5). Consequently, L_1 and L_5 accounted for the effective-flow-paths with both zero-length and non-zero-length CST and DEP.

(3) Segment relief. Profile curvature (*PrCur*) best describes the elevation change along the hillslope and, therefore, was used to determine segment relief in this study. Firstly, midpoints of each segment were determined and these segment midpoints divided the hillslope into six pseudo-segments (Fig. 4). The following equations were derived:

$$z_0 = z_{0,1} + \frac{S_{0,1}L_1}{200} = Z \tag{10}$$

$$z_{i-1,i} = z_{i,i+1} + \frac{S_{i,i+1}(L_i + L_{i+1})}{200} \quad (i = 1, 2, \ldots, 5) \tag{11}$$

$$S_{i-1,i} = S_{i,i+1} - \frac{PrCur_i L_i}{2} \quad (i = 1, 2, \ldots, 5) \tag{12}$$

$$S_{5,6} = \frac{100 z_{4,5}}{L_5/2} \tag{13}$$

where z_0 is the elevation (referenced to the bottom of the hillslope) of the first (highest) point of the hillslope, which equals the total relief (Z) of the hillslope (m); $z_{\text{i}-1,\text{i}}$ is the elevation of the midpoint of segment i (m); $S_{\text{i,i}+1}$ is the slope gradient for the pseudo-segment defined by the midpoints of segment i and segment $i+1$ (%); L_{i} is the length of segment i (m); and $PrCur_{\text{i}}$ is the profile curvature of segment i (unit converted from degree $(100\ \text{m})^{-1}$ to $\%\ \text{m}^{-1}$). The original segments were numbered in sequence (1 to 5) from CST to DEP. Equations 10 to 13 led to:

$$S_{5,6} = \frac{100Z}{L} + \sum_{i=1}^{5}\frac{PrCur_i L_i L_i'}{4L} \tag{14}$$

where Z and L are the total hillslope relief and length, respectively; and L_{i}' is calculated as:

$$L_i' = \begin{cases} L_1 & (i = 1) \\ 2L_1 + L_2 & (i = 2) \\ 2L_1 + 2L_2 + L_3 & (i = 3) \\ 2L - L_4 - 2L_5 & (i = 4) \\ 2L - L_5 & (i = 5) \end{cases} \tag{15}$$

From Eqs. 14 and 15, $S_{5,6}$ can be determined. The elevation of the segment midpoints ($z_{\text{i}-1,\text{i}}$) were then calculated from Eqs. 11 to 13. Elevations of the boundary points for the original segments were linear interpolated from the pseudo-segments (Fig. 4). Thus, the relief of each segment can be determined and slope gradient of each segment were calculated from relief divided by length (Table 4).

Modal Hillslopes

The representative hillslope determined above used mean hillslope length (L_{r2c}) and relief (Z_{r2c}) obtained from the statistical analyses (Table 1). Hillslope length and relief varied considerably within the field as reflected by the percentile values (Table 1). This topographic variability can be described by using a set of two-dimensional hillslopes. In general, hillslope length and relief are positively correlated (i.e., the longer the hillslope, the higher the relief), as demonstrated for the Provost site in Fig. 5a. Consequently, percentile-hillslopes can be established based on the linear regression between hillslope length (L_{r2c}) and relief (Z_{r2c}) calculated for individual points (referred to as the regression method). The percentile value can use either the length scale (L_{r2c}) or the relief scale (Z_{r2c}). For example, using the length scale, length and relief of the 25th percentile hillslope for the Provost site were 100 m (the 25th percentile of L_{r2c}) and 2.7 m (calculated using the regression equation in Fig. 5a), respectively. Alternatively, using the relief scale, length and relief of the 25th percentile hillslope were 81 m (calculated using the regression equation in Fig. 5a) and 2.2 m (the 25th percentile of Z_{r2c}), respectively. These inconsistent results of length and relief scales were mainly due to the nonlinearity between length and relief.

To account for the nonlinearity between length and relief, we used the LS-factor as the scale to determine the percentiles of hillslopes (referred to as the LS-factor method). The flow chart of the LS-factor method is shown in Fig. 6. This method used the hillslope length and relief calculated for each individual point (Table 1) to determine its hillslope slope gradient (S_{r2c}). The hillslope slope gradient and length were used to compute a hillslope LS-factor value using equations for simple linear slopes in the Revised Universal Soil Loss Equation [RUSLE (McCool et al. 1997)]. Percentile values (%) of the hillslope LS-factor were then calculated (Table 1). The hillslope LS-factor percentiles were coupled with their respective hillslope slope gradient percentiles to back calculate hillslope length percentiles, using the same RUSLE LS-factor equations, in reverse. The calculated hillslope length and slope gradient percentiles were used to calculate hillslope relief percentiles. Thus, at each percentile, a hillslope with defined length and relief was established. These percentile-hillslopes were termed modal hillslopes, since the hillslope lengths and reliefs usually did not equal those calculated from individual points at the same percentiles (Table 1). However, they generally followed a similar trend as slope length increased with relief (Fig. 5), although there were exceptions. By using LS-factor as the scale to determine the percentiles, slope length and relief were combined to characterize hydrologic potential of the hillslopes.

It is worth noting that the hillslope LS-factor calculated for a given point must not be interpreted as the LS-factor at that point location (i.e., it cannot be used to calculate water erosion at that point). Instead, it was just one sample of the LS-factor for the hillslopes in the landscape. Consequently, the hillslope LS-factor percentiles were area-weighted values. For example, 25th percentile hillslope LS-factor of the Provost site (0.38, Table 1) can be interpreted as that 25% of the points (area) in the site were located on hillslopes with a LS-factor equal to or less than 0.38.

For each modal hillslope, the segment length was determined as:

$$L_i^x = L^x PL_i/100 \tag{16}$$

where L_i^x is the length of segment i for the xth percentile modal hillslope (m); L^x is the total length of the xth percentile modal hillslope (m); and PL_i is the length percentage of segment i on the representative hillslope (%), which can be calculated from the segment length and total length of the representative hillslope (Table 4).

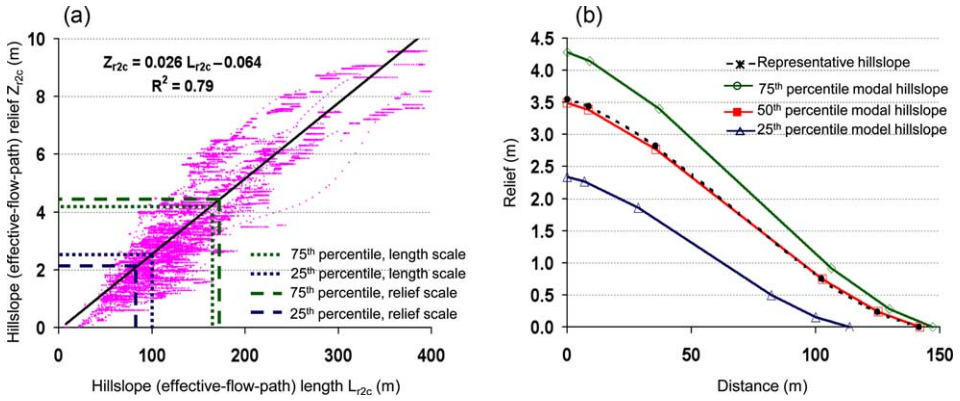

Fig. 5. (a) The correlation between hillslope (effective-flow-path) length and relief; and (b) the representative hillslope and modal hillslopes determined using the LS-factor method (see Fig. 6. for the flow chart of the LS-factor method) for the Provost site. Note that in (b), the greater the length, the higher relief for the modal hillslope, which is similar to the trend shown in (a).

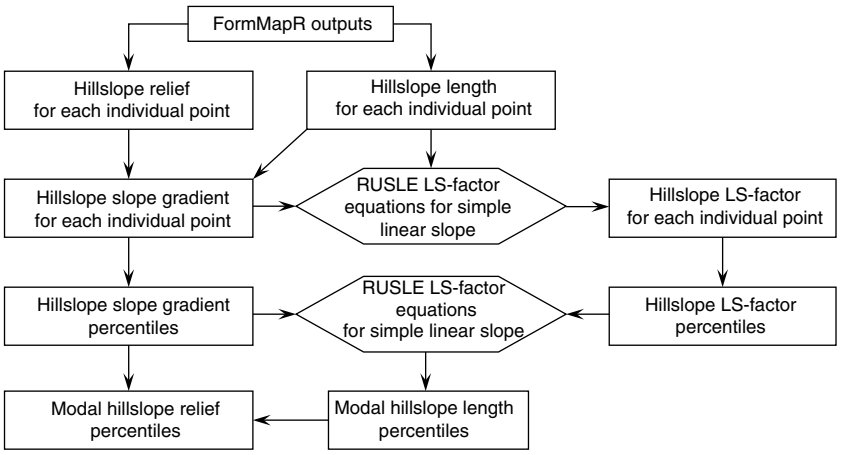

Fig. 6. Flow chart for the LS-factor method used to determine the percentile modal hillslopes. The quartile modal hillslopes for the Provost site are shown in Fig. 5(b).

Segment relief of each modal hillslope was determined following the same procedures used for the representative hillslope (i.e., Eqs. 10 to 15). Three model hillslopes for the Provost site are shown in Fig. 5b.

Topographic Complexity Indices

Divergence and convergence resulted in differences between area percentage (PA) and length percentage (PL) for the same landform elements (hillslope segments) (Fig. 2). Test runs showed that these differences increased when divergence or convergence increased. In other words, the magnitude of the difference between PA and PL is an indication of the degree of divergence or convergence. Consequently, we developed a topographic complexity index (TCI) to quantify the degrees of divergence and convergence based on the differences between PA and PL.

The first step was to combine the five landform elements into three major landform elements: upper-slope (CST and UPS), middle-slope (MID) and lower-slope (LOW and DEP). Two diverse scenarios were assessed: the first was a landscape with no divergence or convergence, for which there was no difference between PA and PL for any major landform elements (Fig. 3a); the second scenario was a landscape with the highest divergence and convergence, for which, PL was greater than PA in upper-slope and lower-slope, but was less than PA in middle-slope (Fig. 3b). Most landscapes are between these two extreme scenarios (Fig. 3c). Theoretically, a given landscape can be generalized as a combination of the two extreme scenarios (Fig. 3d), consisting of a rectangular component (representing the no divergence or convergence scenario) and a triangular component (representing the highest divergence and convergence scenario). The triangular component was fixed, whereas the rectangular component varied in width, depending on the degree of divergence and convergence. The topographic complexity index was derived separately for the upper- and lower-slope. For the upper-slope, let:

$$\alpha = \frac{A^T}{A} = \frac{A^T}{A^R + A^T} \tag{17}$$

where A^{R} and A^{T} are the areas of the rectangular and triangular components, respectively, and A is the total area (Fig. 3d). As a result:

$$w = \frac{H}{4}\left(\frac{1}{\alpha} - 1\right) \tag{18}$$

$$\frac{PA_u}{100} = \frac{A_u}{A} = \frac{A_u^R + A_u^T}{A} = \frac{wL_u + ((\pi(L_u)^2)/8)}{(H^2)/(4\alpha)}$$

$$= (1-\alpha)\frac{L_u}{H} + \frac{\pi\alpha}{2}\left(\frac{L_u}{H}\right)^2 \tag{19}$$

where PA is the area percentage, H and w are the height and width of the rectangular component, respectively and subscript u denotes the upper-slope (Fig. 3d). Length percentage (PL) for the rectangular component was calculated from:

$$\frac{PL_u^R}{100} = \frac{L_u}{H} \tag{20}$$

For the triangular component, PL was approximated with a flow path through the central point (Fig. 3d) determined as:

$$\frac{PL_u^T}{100} = k\frac{L_u}{H} \tag{21}$$

where

$$k = 2/\sqrt{10 - 4\sqrt{2}} \tag{21-1}$$

The overall length percentage was calculated as the area-weighted average of the rectangular and triangular components:

$$\frac{PL_u}{100} = (1-\alpha)\frac{PL_u^R}{100} + \alpha\frac{PL_u^T}{100} = (1-\alpha+k\alpha)\frac{L_u}{H} \quad (22)$$

Eqs. 19 and 22 together yield:

$$\alpha = \frac{c_2}{2c_1} - \sqrt{\frac{c_2^2}{4c_1^2} - \frac{c_3}{c_1}} \quad (23)$$

where

$$c_1 = 2PL_u - 2kPL_u - 2k^2PA_u + 4kPA_u - 2PA_u \quad (23\text{-}1)$$

$$c_2 = \pi PL_u^2 - 4PL_u + 2kPL_u - 4kPA_u + 4PA_u \quad (23\text{-}2)$$

$$c_3 = 2PL_u - 2PA_u \quad (23\text{-}3)$$

The topographic complexity index for the upper-slope (TCI_u) was defined as:

$$TCI_u = 100\alpha \quad (24)$$

The topographic complexity index for the lower-slope (TCI_l) was determined similar to the upper-slope with values for the upper-slope replaced by those for the lower-slope (Eqs. 17 to 24). The overall topographic complexity index for the landscape (TCI) was calculated as the area-weighted average of TCI_u and TCI_l as:

$$TCI = (PA_u TCI_u + PA_l TCI_l)/(PA_u + PA_l) \quad (25)$$

The values of these topographic complexity indices were scaled from 0 to 100% and represented the areal percentages of the triangular component (Eqs. 17, 24 and 25). Therefore, the scenario with no divergence or convergence has a TCI of zero, corresponding to a rectangular component of infinite width (Fig. 3a, d), whereas the scenario with the highest divergence and convergence has a TCI value of 100, corresponding to a rectangular component with zero width (Fig. 3b, d).

In summary, the values of TCIs are derived from the area and length percentages of the combined upper-slope and lower-slope segments, which in turn are determined by the terrain analyses and landscape segmentation. The TCI values increase with the degree of divergence or convergence and, therefore, provide quantitative measures to indicate the topographic complexities for the DEM as a whole. Test runs with sites in the previous study by MacMillan and Pettapiece (2000) showed that values of TCI indices normally ranged between 10% and 60% (data not presented), indicating that most landscapes have some degree of divergence and convergence, but rarely as high as in the scenario shown in Fig. 3b. Furthermore, many sites showed relatively symmetric divergence and convergence with similar values of TCI_u and TCI_l, although for some sites, they were markedly different. The values for the Provost site are shown in Table 5. Overall, these TCI values indicate that the Provost site has substantial degrees of divergence and convergence with the magnitude of convergence in lower-slopes higher than the magnitude of divergence in upper-slopes. This analysis is consistent with visual observations of flow paths (Fig. 1a).

Other Aspects of Landscape Topography

Additional parameters and ratios can be derived and used to reflect various aspects of the landscape topographic characteristics (Table 5). Some of these parameters and ratios may be used as inputs to agri-environmental models and could be useful in relating different agri-environmental processes. For example, average watershed area (A_{ws}), watershed density (D_{ws}) and channel density (D_c) are commonly used in

Table 5. Topographic complexity indexes and other parameters and ratios characterizing different aspects of landscape topography

Parameter	Symbol	Calculation	Aspect of topographic characteristic	Value[z]
Upperslope topographic complexity index (%)	TCI_u	Eqs. 17 to 24	Divergence on upper-slope (CST and UPS) area	36
Lowerslope topographic complexity index (%)	TCI_l	Eqs. 17 to 24 with values for upper-slope replaced by those for lower-slope	Convergence on lower-slope (LOW and DEP) area	47
Landscape topographic complexity index (%)	TCI	Eq. 25	Divergence and convergence of the landscape	42
Average watershed area (ha)[y]	A_{ws}	Total area/the number of watersheds	Watershed development, watershed size	3.9
Watershed density (count (100 ha)$^{-1}$)[y]	D_{ws}	$100/A_{ws}$	Watershed development, watershed size	25.6
Ridge density (m ha^{-1})	D_r	Total ridge length[x]/total area	Ridge development	46
Channel density (m ha^{-1})	D_c	Total channel length[x]/total area	Channel development	36
Percent off-site drainage (%)[y]	P_{osd}	Area of edge watersheds/total area	Connection to outside world	31
Maximum relief (m)	Z_{max}	Maximum elevation – minimum elevation	Range of relief	15.3
Landscape flow path relief ratio	RZ_l	Z_{max}/Z_{p2p}	Watershed development, larger scale trend	2.2
Watershed flow path relief ratio	RZ_w	Z_{p2p}/Z_{r2c}	Channel development	1.9
Watershed flow path length ratio	RL_w	L_{p2p}/L_{r2c}	Channel development	2.2

[z]Value calculated for the Provost site.
[y]Small edge watersheds are eliminated from the calculation.
[x]Approximated by the product of point counts and cell size.

hydrology. Another example is percent off-site drainage (P_{osd}), which can be used to link landscape processes to larger scale hydrologic systems (e.g., investigating the effect of land management on stream water quality). It is worth noting that A_{ws}, D_{ws} and P_{osd} are strongly affected by boundary effect, i.e., many small edge watersheds were incomplete watersheds (Fig. 1a, d). To reduce the boundary effect, edge watersheds (with at least one point at the edges of the DEM) were separated from the non-edge watersheds (with no point at the edges of the DEM). Edge watersheds with an area less than the tenth area percentile of the non-edge watersheds were considered incomplete watersheds and removed from the calculations.

The landscape flow path relief ratio (RZ_l) was calculated as the maximum relief of the DEM (Z_{max}) divided by the average full-flow-path (peak to pit) relief (Z_{p2p} in Table 1). A landscape with high RZ_l value likely has a larger scale topographic trend superimposed onto the field-scale topographic pattern. The watershed flow path relief ratio (RZ_w) and length ratio (RL_w) were calculated as the average full-flow-path relief and length (Z_{p2p} and L_{p2p} in Table 1, respectively) divided by, respectively, the average effective flow path (ridge to channel) relief and length (Z_{r2c} and L_{r2c} in Table 1, respectively). They indicate the complexity of the within-watershed channel network, in particular, the development of channels upslope towards the peak (e.g., through headcut). Landscapes with complex within-watershed channel network or with channels developed further upslope often have high RZ_w and RL_w values.

Applications of the Methodology and the Quantitative Topographic Data

In the SLC database, a SLC polygon normally will have multiple soils, each assigned with a landform (landform type and slope class) and an area percentage (AAFC 2007). This provides the topographic context of soils in the SLC polygon. The methodology developed in this study will be applied on representative sites across Canada with landforms typical of Canadian agricultural landscapes. The goal is to establish a comprehensive topographic model for each landform in the SLC database. With these comprehensive topographic models, the nominal topographic information in the SLC database (landform) can be converted into quantitative topographic data. Consequently, the tacit knowledge stored in the SLC database (i.e., the topographic context of soils) can be expressed quantitatively, which provides agri-environmental modelers more realistic soil and topographic input data.

The full potential of the various topographic data provided with this methodology in agri-environmental modeling is yet to be explored. However, the use of some key topographic data is promising. For example, soil erosion models such as the RUSLE and Water Erosion Prediction Project (WEPP) use a two-dimensional hillslope as topographic input data. With a set of modal hillslopes, one can obtain not only overall average soil erosion rates, but also percentile soil erosion rates at different slope positions. Together, the average and percentile soil erosion rates provide a measure of the variability (uncertainty) of soil erosion due to topography. Some topographic characteristics may be useful in refining the modeling results. For example, tillage can cause translocation of soil in directions along and perpendicular to the tillage direction. Topographic data in both directions are needed for accurate estimation of tillage erosion (e.g., Li et al. 2008). A two-dimensional hillslope only provides topographic data in one horizontal direction. Topographic Complexities Indices can be used to approximate the topographic data perpendicular to the two-dimensional hillslopes, thereby, provide more realistic tillage erosion rates. Moreover, some topographic characteristics can be used to build connections between different processes. As mentioned earlier, percent off-site drainage can be used to estimate how much eroded soil is being delivered to the outside world, i.e., streams or waterbodies, linking soil erosion to water quality assessment.

It should be noted that the methodology developed in this study was not designed for digital soil mapping (DSM), although some topographic characteristics may be useful in delineating soil units. There were similarities between the approaches used for the terrain analysis and landscape segmentation in this study and the approaches used for predicting soil properties or delineating soil units in some DSM studies (e.g., Zhu et al. 1997, 2001, 2010; Grunwald 2009; Qin et al. 2009; Shi et al. 2010). The difference was that with the methodology developed in this study, topography of the DEM as a whole was summarized and characterized (e.g., by the modal hillslopes), whereas in those DSM studies, topographic information was used to determine soil properties at unknown points or to draw boundaries between different soil units. Also, the methodology was developed on fine resolution DEMs (point interval typically in the range of 1–20 m). Further studies are needed to examine the applicability of this methodology on coarse resolution DEMs (e.g., point interval >30 m).

CONCLUSIONS

A methodology was developed in this study to derive various topographic derivatives from fine resolution DEMs and to classify landscapes into elements with distinct topographic characteristics. Data obtained from these analyses, in particular, the average ridge-to-channel length and relief, the profile curvature and area and length percentages of each landform element (hillslope segment) can be used to calculate a representative two-dimensional hillslope with defined length and slope gradient for each segment. A set of two-dimensional modal hillslopes can be developed to describe the variability of topography in three dimensions. Topographic complexity indices can be developed from these analyses as a quantitative measure of the

degrees of divergence and convergence for upper- and lower-slopes, respectively, and for the landscape as a whole. Additional topographic parameters, ratios and indices can be calculated to characterize topography and to provide inputs to agri-environmental models. The methodology developed in this study provides a means to obtain quantitative topographic data that can be used in agri-environmental models through analyses of representative sites for landforms typical of Canadian agricultural landscapes.

ACKNOWLEDGEMENTS

Financial support for this study was provided by the Agriculture and Agri-Food Canada (AAFC) through the National Agri-Environmental Health Analysis and Reporting Program (NAHARP) as part of the project entitled "Developing and validating the Soil Erosion Risk Indicator (SoilERI) for the use on agricultural land in Canada". The authors thank S. Smith, W. Eilers and A. Lefebvre from Agriculture and Agri-Food Canada for their continuous support. We are grateful to the two anonymous reviewers for their insightful comments.

Agriculture and Agri-Food Canada. 2007. Soil landscape of Canada (SLC). Version 3.1.1. 1:1,000,000 scale digital soil map for the agricultural regions of Canada. Canadian Soil Information System, Ottawa, ON.

Band, L. E. 1986. Topographic partitioning of watersheds with digital elevation data. Water Resour. Res. **22**: 15–24.

Brady, N. C. and Well, R. R. 2002. The nature and properties of soils. 13th ed. Pearson Education Inc., Upper Saddle River, NJ. pp. 61–62.

Burrough, P., MacMillan, R. and van Deursen, W. 1992. Fuzzy classification methods for determining land suitability from soil profile observations and topography. J. Soil Sci. **43**: 193–210.

Burrough, P., van Gaans, P. and MacMillan, R. 2000. High-resolution landform classification using fuzzy k-means. Fuzzy Sets and Systems **113**: 37–52.

Foster, G. R. 2004. Draft science documentation. Revised Universal Soil Loss Equation Version 2. pp. 23–29. [Online] Available: http://www.ars.usda.gov/SP2UserFiles/Place/64080530/RUSLE/RUSLE2_Science_Doc.pdf, [2006 Dec. 12].

Grunwald, S. 2009. Multi-criteria characterization of recent digital soil mapping and modeling approaches. Geoderma **152**: 195–207.

Irwin, B. J., Ventura, S. J. and Slater, B. K. 1997. Fuzzy and isodata classification of landform elements from digital terrain data in Pleasant Valley, Wisconsin. Geoderma **77**: 137–154.

Kirkby, M. J., Irvin, B. J., Jones, R. J. A., Govers, G. and The PESERA Team. 2008. The PESERA coarse scale erosion model for Europe. I. Model rationale and implementation. Eur. J. Soil Sci. **59**: 1293–1306.

Lefebvre, A., Eilers, W. and Chunn, B., eds. 2005. Environmental sustainability of Canadian agriculture: Agri-Environmental Indicator Report Series – Report #2. Agriculture and Agri-Food Canada, Ottawa, ON. 220 pp.

Li, S., Lobb, D. A., Lindstrom., M. J. and Farenhorst, A. 2008. Patterns of tillage and water erosion on topographically complex landscapes in the North America Great Plains. J. Soil Water Cons. **63**: 37–46.

Li, S., Lobb, D. A., Kachanoski, R. G. and McConkey, B. G. 2010. Comparing the use of the traditional and repeated-sampling-approach of the ^{137}Cs technique in soil erosion estimation. Geoderma. **160**: 324–335.

MacMillan, R. A. 2003. LandMapR Software Toolkit- C++ Version: Users manual. LandMapper Environmental Solutions Inc., Edmonton, AB. 110 pp.

MacMillan, R. A., Martin, T. A., Earle, T. J. and McNabb D. H. 2003. Automated analysis and classification of landforms using high-resolution digital elevation data: applications and issues. Can. J. Remote Sensing **29**: 592–606.

MacMillan, R. A. and Pettapiece, W. W. 2000. Alberta landforms: Quantitative morphometric descriptions and classification of typical Alberta landforms. Agriculture and Agri-Food Canada, Research Branch, Semiarid Prairie Agricultural Research Centre, Swift Current, SK. Technical Bulletin No. 2000–2 E. 118 pp.

MacMillan, R. A., Pettapiece, W. W., Nolan, S. C. and Goddard, T. W. 2000. A generic procedure for automatically segmenting landforms into landform elements using DEMs, heuristic rules and fuzzy logic. Fuzzy Sets and Systems **113**: 81–109.

McConkey, B. G., Monreal, C. M., Huffman, T., Patterson, G. T., Brierley, J. A., Desjardins, R. L., Rochette, P., Carter, M. R., Bentham, M. and Gameda, S. 2003. National carbon and greenhouse-gas emission accounting and verification system for agriculture (NCGAVS). Pages 79–92 *in* C. A. S. Smith, ed. Soil organic carbon and agriculture: Developing indicators for policy analyses. Proc. OECD Expert Meeting, Ottawa, ON, Canada. Agriculture and Agri-Food Canada, Ottawa, ON, and Organisation for Economic Co-operation and Development, Paris.

McCool, D. K., Foster, G. R. and Weesies, G. A. 1997. Slope length and steepness factors (LS), Chapter 4, pages 101–141 *in* K. G. Renard, G. R. Foster, G. A. Weesies, D. K. McCool, and D. C. Yoder, eds. 1997. Predicting soil erosion by water: a guide to conservation planning with the Revised Universal Soil Loss Equation (RUSLE). Agriculture Handbook No. 703. U.S. Department of Agriculture, Agricultural Research Service, Washington, DC. 404 pp.

Moore, I. D., Gessler, P. E., Neilsen, G. A. and Peterson, G. A. 1993. Soil attribute prediction using terrain analysis. Soil Sci. Soc. Am. J. **57**: 443–452.

Pennock, D. J. and Corre, M. D. 2001. Development and application of landform segmentation procedures. Soil Tillage Res. **58**: 151–162.

Pennock, D. J., Zebarth, B. J. and de Jong, E. 1987. Landform classification and soil distribution in hummocky terrain, Saskatchewan, Canada. Geoderma **40**: 297–315.

Pennock, D. J., Anderson, D. W. and de Jong, E. 1994. Landscape changes in indicators of soil quality due to cultivation in Saskatchewan, Canada. Geoderma **64**: 1–19.

Qin, C., Zhu, A., Shi, X., Li, B., Pei, T. and Zhou, C. 2009. Quantification of spatial gradation of slope positions. Geomorphology **110**: 152–161.

Rochette, P., Worth, D. E., Lemke, R. L., McConkey, B. G., Pennock, D. J., Wagner-Riddle, C. and Desjardins, R. L. 2008. Estimation of N_2O emissions from agricultural soils in Canada. I. Development of a country-specific methodology. Can. J. Soil. Sci. **88**: 641–654.

Shi, X., Long, R., Dekett, R. and Philippe, J. 2010. Integrating different types of knowledge for digital soil mapping. Soil Sci. Soc. Am. J. **73**: 1682–1692.

Soil Classification Working Group. 1998. The Canadian system of soil classification. Agriculture and Agri-Food Canada, Ottawa, ON. Publ. 1646 (revised). 187 pp.

Wilson, J. P. and Gallant, J. C. 2000. Digital terrain analysis. Pages 1–27 *in* J. P. Wilson and J. C. Gallant, eds. Terrain analysis: Principles and applications. John Wiley, New York, NY.

Zhu, A., Band, L., Vertessy, R. and Dutton, B. 1997. Derivation of soil properties using a soil land inference model (SoLIM). Soil Sci. Soc. Am. J. **61**: 523–533.

Zhu, A., Hudson, B., Burt, J. E. and Lubich, K. 2001. Soil mapping using GIS, expert knowledge and fuzzy logic. Soil Sci. Soc. Am. J. **65**: 1463–1472.

Zhu, A., Qi, F., Moore, A. and Burt, J. E. 2010. Prediction of soil properties using fuzzy membership values. Geoderma **158**: 199–206.